AGU PUBLICATIONS

Geophysical Research Letters

RESEARCH LETTER

10.1002/2015GL065259

**Key Points:**
- $^{134}$Cs was observed at 174.3°W in 2012 and the signal extended to 160.6°W by 2013
- No $^{134}$Cs was detected east of 152°W
- $^{134}$Cs penetration progressively shoals toward east

**Supporting Information:**
- Supporting Information S1
- Figure S1
- Table S1

**Correspondence to:**
S. Yoshida,
syoshida@whoi.edu

**Citation:**
Yoshida, S., A. M. Macdonald, S. R. Jayne, I. I. Rypina, and K. O. Buesseler (2015), Observed eastward progression of the Fukushima $^{134}$Cs signal across the North Pacific, *Geophys. Res. Lett.*, *42*, 7139–7147, doi:10.1002/2015GL065259.

Received 8 JUL 2015
Accepted 7 AUG 2015
Accepted article online 11 AUG 2015
Published online 9 SEP 2015



# Observed eastward progression of the Fukushima $^{134}$Cs signal across the North Pacific

**Sachiko Yoshida[1], Alison M. Macdonald[1], Steven R. Jayne[1], Irina I. Rypina[1], and Ken O. Buesseler[1]**

[1]Woods Hole Oceanographic Institution, Woods Hole, Massachusetts, USA

**Abstract** Radionuclide samples taken as part of hydrographic surveys at 30°N in the North Pacific reveal that the easternmost edge of Fukushima-derived $^{134}$Cs observed at 174.3°W in 2012 had progressed eastward across the basin to 160.6°W by 2013. The 2013 30°N observations indicate surface $^{134}$Cs concentrations of 3–5 Bq/m$^3$ between 160°E and 160°W, slightly lower concentrations west of 160°E and no detectable signal east of 160.6°W. Profile samples show $^{134}$Cs penetration to 500 m west of 180° with shoaling penetration depth toward to the east. The near-uniform vertical distribution of $^{137}$Cs between 152°W and 121.3°W in the top 500 m is indicative of trace amounts of radionuclides remaining from weapons testing. The physical processes responsible for the deep $^{134}$Cs penetration in the western Pacific appear to be related to distinct water mass subduction pathways; however, the timing and rapidity of deep penetration over the broad scales observed has yet to be clarified.

## 1. Introduction

A substantial quantity of radionuclides was released to the atmosphere and discharged into the North Pacific Ocean in the spring of 2011 during the Fukushima nuclear power plant (FNPP) accident. Starting a few days after the 11 March tsunami, overheating at the FNPP led to an explosive release of gases and volatiles to the atmosphere, which were deposited as fallout. It was estimated that 70–80% of the discharge to atmosphere was deposited over the ocean [*Yoshida and Kanda*, 2012]. The direct discharge to the ocean of radioactive waters from emergency cooling waters and groundwater peaked on 6 April 2011 [*Buesseler et al.*, 2011]. Orders of magnitude lower discharges of cesium continue to this day via groundwater and river discharge [*Kanda*, 2013; *Nagao et al.*, 2013]. Studies reporting the total magnitude of the FNPP release to the environment present a substantial range in no small part due to the range in estimates for total $^{137}$Cs entering the ocean which range from about 3.5 to 53 PBq, with equal amounts of $^{134}$Cs [*Chino et al.*, 2011; *Stohl et al.*, 2012; *Bailly du Bois et al.*, 2012; *Tsumune et al.*, 2012; *Charette et al.*, 2013; *Rypina et al.*, 2013; *Miyazawa et al.*, 2013].

The FNPP is located at approximately 141.0°E, 37.4°N in an oceanographically active region between the subtropical and subpolar gyres. In the western North Pacific, the Kuroshio, a subtropical gyre western boundary current, brings warm water from the tropics and the subtropics northward along the continental slope of Japan carrying some 60–80 sverdrup ($10^6$ m$^3$/s) [*Worthington and Kawai*, 1972; *Imawaki et al.*, 2001; *Book et al.*, 2002; *Macdonald et al.*, 2009]. The Oyashio is the southward flowing western boundary current of the Western Subarctic Gyre. The FNPP is situated slightly north of the Kuroshio separation point on the northeast coast of Japan's Bōsō Peninsula at ~35°N and south of the Oyashio's entrance into the Pacific on the eastern side of Kuril Islands at ~45.5°N. This particular location meant that once beyond the continental shelf, FNPP contaminated waters entered the Kuroshio and Oyashio confluence region characterized by strong currents and eddy mixing. The importance of the Kuroshio and its associated eddies was revealed by one of the earliest surveys in June 2011, showing that the location of the highest Fukushima-derived Cs concentration coincided with the near-shore eddies, while nondetectable Cs levels were observed to the south of the Kuroshio [*Buesseler et al.*, 2012]. Flowing eastward with the energetic, highly variable inertial jet, the contaminated water mass was strongly influenced by both the meanders and mesoscale eddies in the Kuroshio Extension (KE) [e.g., *Rypina et al.*, 2013].

In the 3 years since the accident, water samples at various locations have been collected by a number of different research groups and are currently being analyzed to determine the breadth and timing of horizontal propagation and the depth of the vertical penetration of radionuclides into the North Pacific Ocean. It has taken both time and resources for in situ water sampling to develop a database of observations capable of

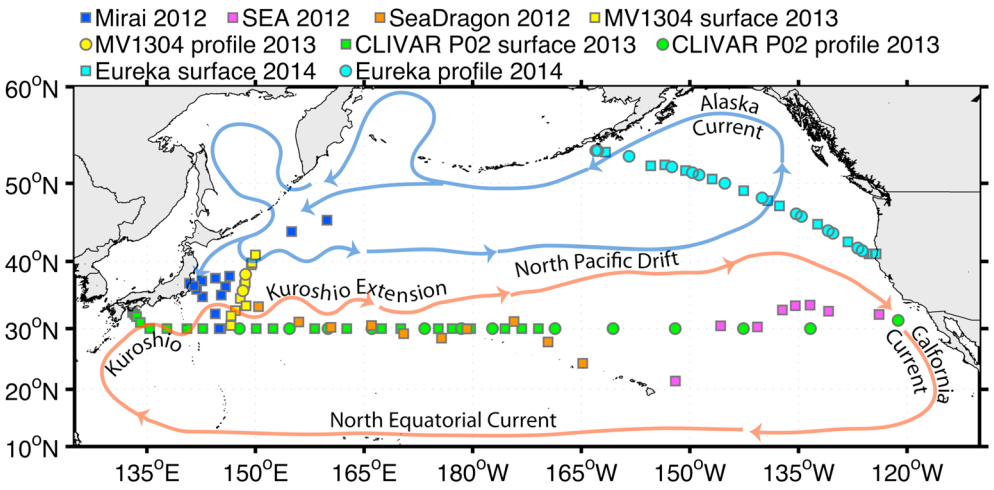


**Figure 1.** The 2012–2014 sampling locations, color coded by expedition. Squares and circles denote surface and profile sampling locations, respectively. Blue and orange arrows schematically illustrate the pathway of the mean surface currents in the North Pacific subpolar and subtropical gyres.

capturing the widespread distribution of FNPP radionuclides, including its vertical structure. In the meantime, numerical modeling has been widely used to predict the location and the level of contamination from the FNPP. In the coastal regions, several model simulations suggest that shortly after the major discharge event, the transport pathway of the radionuclides was strongly influenced by the coastal currents and near-shore eddies, which led to relatively fast exchanges between contaminated and uncontaminated waters [*Miyazawa et al.*, 2013; *Masumoto et al.*, 2012]. This result was supported by in situ Cs observations [*Buesseler et al.*, 2012] and surface drifters deployed within 400 km of FNPP, which showed the majority of trajectories leaving coastal regions to be advected into the subtropical gyre circulation on a time scale of weeks to months [*Rypina et al.*, 2013].

Numerical tracer simulations indicate that the long-term (years to a decade) evolution of the horizontal advection of Fukushima-contaminated waters is strongly affected by the interaction with mesoscale eddies and current instabilities, which increase the dilution of contaminants. Generally, numerical simulations suggest that the bulk of the tracer moved eastward following the surface currents in the North Pacific, crossing the basin from Japan to the U.S. West Coast in about 3–5 years, and penetrating vertically to depths of 200 to 600 m [*Rossi et al.*, 2013, 2014; *Behrens et al.*, 2012]. Similar travel times across the basin were also indicated by historical surface drifter data [*Rypina et al.*, 2014]. Detection of FNPP Cs has recently been reported on the Canadian continental shelf with concentrations of about 2 $Bq/m^3$ in the upper 150 m [*Smith et al.*, 2014]. Here using Cs concentration estimates from water samples collected on oceanographic expeditions occupied from 2012 to 2014, we present observational findings that describe the propagation and spatial distribution of Fukushima-derived Cs isotopes in the North Pacific 1–3 years after discharge.

## 2. Data and Analysis Method

The Cs observations analyzed in this study consist of 78 surface and 30 profile samples collected from six cruises occupied from 2012 to 2014 (Figure 1). Relatively speaking, the far western basin is better sampled, with a greater number of observations available near Japan and fewer over the broader region of the central and eastern Pacific. In 2012, surface water samples were collected along a section occupied by the Sea Dragon Cruise (operated by the Two Hands Project: www.twohandsproject.org) from Yokohama to Hawaii (June to July 2012) and along the Plastics at Sea section occupied by the sailing school vessel Robert C. Seamans (operated by the Sea Education Association: www.sea.edu) from San Diego to Hawaii (October to November 2012).

In 2013, samples were collected along the 30°N–40°N meridional line just west of 150°E by the University of Washington student cruise, MV1304 (March 2013), and along the basin-wide 30°N transect (P02) conducted as part of the U.S. Climate Variability and Predictability (CLIVAR) program (March–May 2013). In addition to

the surface samples, these 2013 data sets included two upper water column profiles obtained by the MV1304 cruise and 13 deeper vertical profiles collected as part of P02. The P02 profiles consist of samples from four different depth ranges, nominally, (a) surface (30–45 m), (b) subsurface (100–200 m), (c) intermediate (250–350 m), and (d) deep (450–550 m). Note that while the "surface" samples from most of cruises were collected from the upper a few meter of water column, P02 nonprofile surface samples (different from the shallowest profile samples a) were intentionally collected from about 65 m to take into account the depth of the springtime mixed layer depth estimated from Argo floats [*Holte and Talley*, 2009].

At the end of July through the beginning of August 2014, samples were collected on the R/V *Point Sur* operated by the Moss Landing Marine Laboratory (MLML; https://www.mlml.calstate.edu/) along the transect from Dutch Harbor to Eureka crossing the Alaskan gyre. These MLML samples included 15 surface and 15 profile samples with 6 samples collected from 600 m depth.

All the samples were analyzed onshore in the lab using one of two resin-based methods: ammonium molybdophosphate on an organic polymer polyacrylonitrile or potassium-nickel hexacyanoferrate (II) [*Šebasta and Štefula*, 1990; *Kamenik et al*., 2013; *Pike et al*., 2013]. Two cesium radioisotopes, $^{134}$Cs (half-life of 2.06 years) and $^{137}$Cs (half-life of 30.07 years) are used in this study to examine radionuclides derived from Fukushima. The $^{137}$Cs isotope is known to have preexisted in the global oceans prior to the FNPP accident as a result of the weapons testing experiments that peaked in the 1960s [*Bowen et al*., 1980; *United Nations*, 2000]. By 2011, after decades of ocean mixing and dispersion, the distribution of surface weapons-based $^{137}$Cs concentration was nearly uniform throughout the North Pacific, with values of 1.5–2.0 Bq/m$^3$ [*Aoyama and Hirose*, 2004; *Aoyama et al*., 2011; *Inomata et al*., 2009]. The $^{134}$Cs isotope, on the other hand, is unique to the FNPP release with no significant anthropogenic $^{134}$Cs remaining in the ocean prior to the 2011 accident due to its short half-life. As it is known that the ratio of $^{134}$Cs/$^{137}$Cs from the FNPP contamination was close to 1.0 [*Buesseler et al*., 2012], any detectable level of $^{134}$Cs allows us to distinguish the Fukushima-origin $^{137}$Cs from preexisting sources. The results reported here are based on concentration decay corrected to the major liquid discharge event date on 6 April 2011 [*Buesseler et al*., 2011]. All sampling locations and Cs concentration are provided in Table S1 in the supporting information.

## 3. Surface Concentration and an Eastern Edge of the Fukushima Signal

Based on the observations described in preceding section, from 2012 to 2014, the $^{134}$Cs concentrations reflecting FNPP contaminated waters ranged between 0.5 and 10 Bq/m$^3$ everywhere except for two locations with the higher activities near Japan (Figure 2). At these two sites, samples collected from the R/V *Mirai* 2012 cruise indicate the concentrations of 42.9 Bq/m$^3$ at 140.9°E, 36.9°N and 14.7 Bq/m$^3$ at 141.5°E, 36.5°N. Both sites are located just south of the FNPP within a distance of 100 km from the plant. Such high concentrations a year after the accident are likely due to the continued discharge [*Kanda*, 2013]; a conclusion that is further supported by the fact that the distribution of cesium close to the FNPP is spatially inhomogeneous and fluctuates on short time scale due to the transient variability of coastal currents. Therefore, it is to be expected that the observed values, while sensitive to the discharge, also depend on the exact time and location at which water samples were taken. Repeat water samples collected near the same site in 2012 and 2013 suggest generally decreasing Cs concentrations with some fluctuation on the observed time scales. At one repeat station located at 141.0°E, 36.5°N, for example, the $^{134}$Cs concentration was reported as 77.5 Bq/m$^3$ in May 2012, while a year later it had decreased to 1.0 Bq/m$^3$, with a further decrease to below the detection limit (0.2 Bq/m$^3$) by September 2013 (data available at http://www.ourradioactiveocean.org/results.html).

In 2012, the easternmost location of detectable $^{134}$Cs was 174.3°W with the concentration of 3.8 Bq/m$^3$ at 31.1°N (Figure 2A). In 2013, the easternmost edge of the $^{134}$Cs plume had progressed further eastward to 160.6°W, 30.0°N, where the observed $^{134}$Cs concentration was 2.8 Bq/m$^3$ (Figure 2B). All stations located east of 160.6°W showed no evidence of $^{134}$Cs arrival as of 2013. Fukushima radionuclides were discharged from FNPP at a latitude of about 37°N, and according to both modeling [*Rossi et al*., 2013, 2014; *Behrens et al*., 2012; *Garraffo et al*., 2014] and observation-based [*Rypina et al*., 2013] studies, the main plume was initially advected eastward along the KE. While contamination stayed mostly on northern side of the strong KE in the western basin, the plume began to spread across the current axis as it moved eastward, eventually following the North Pacific Drift in the eastern Pacific (Figure 1, orange arrows). Located south of the KE axis at

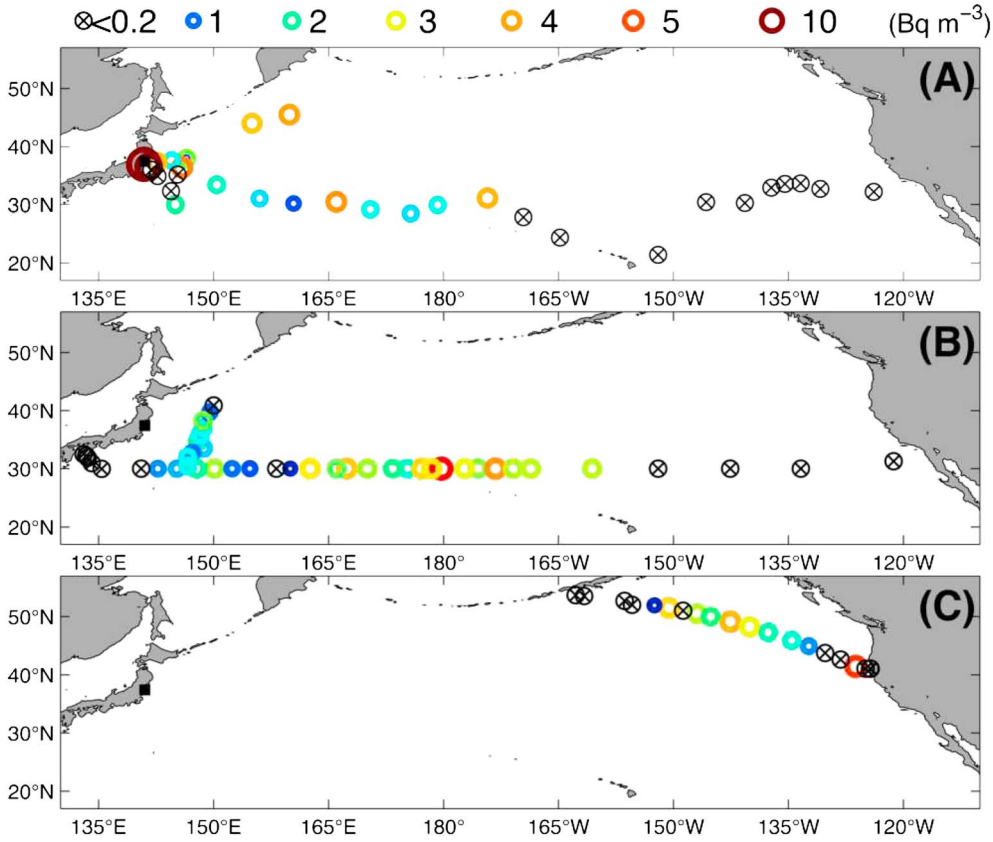


**Figure 2.** North Pacific surface $^{134}$Cs concentration in (A) 2012, (B) 2013, and (C) 2014. Concentrations indicated by both circle size and color. Circles with crosses indicate concentrations below the detection limit (<0.2 Bq/m$^3$). These surface values include all the shallowest observations from the available data sets including both surface and profile samples. Units: Bq/m$^3$.

about 34°N, the P02 line at 30°N is not aligned with the center of the $^{134}$Cs plume but is expected to intersect the southern edge of the main plume where the surface eastward flow is slower and less coherent. Based on the locations of the 2012 and 2013 easternmost $^{134}$Cs observations, the leading edge of the eastward progression of the surface $^{134}$Cs signal along the 30°N in the central Pacific is estimated to have been about 15° of longitude/year (~5 cm/s). This speed for the Cs plume is of the same order as that estimated from independent observational data [*Aoyama et al*., 2013]. The eastward progression of the observed $^{134}$Cs from 2012 to 2013 along 30°N is also consistent with but slightly slower than the estimates based on the historical drifters passing near Fukushima and traveling into the North Pacific [*Rypina et al*., 2014] and numerical model simulation estimates that suggest tracer arrival to the east of 170°W at 30°N by June 2012 [*Rossi et al*., 2013, 2014; *Behrens et al*., 2012; *Garraffo et al*., 2014].

Samples taken along the zonal line at 30°N (Figure 2B) indicate that in 2013 the surface $^{134}$Cs concentration in the central Pacific (160°E–160°W, green to red circles) was a few Bq/m$^3$ higher than in the western Pacific (west of 160°E, blue to green circles). These higher midbasin concentrations of surface $^{134}$Cs concentrations from 3 to 5 Bq/m$^3$ imply that the bulk of the $^{134}$Cs plume originating from the major discharge event in early April 2011 was spread between ~160°E and ~160°W by May 2013. Isotopes of $^{134}$Cs within the Kuroshio at the southeast coast of Japan and the Kuroshio bifurcation off the Bōsō Peninsula were below the detection level (<0.2 Bq/m$^3$, black circled crosses). Along the meridional transect near 150°E across the KE front (30°–40°N), samples contained about 1 to 2 Bq/m$^3$ of $^{134}$Cs and showed no significant north-south gradient in concentration across the KE front. The pronounced difference in the observed $^{134}$Cs distribution across the Kuroshio in 2013 (generally 1 to 2 Bq/m$^3$) compared to that seen in 2011 survey (3 to 3000 Bq/m$^3$ [*Buesseler et al*., 2012]) suggests that 2 years of dilution processes supported by ocean mixing and horizontal advection are well on

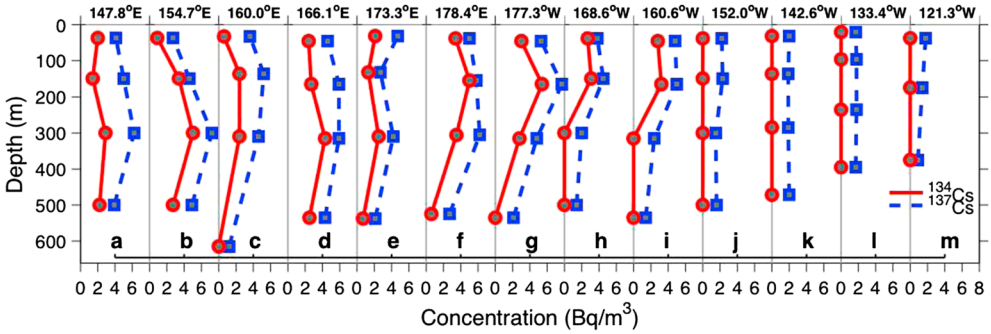


**Figure 3.** Profiles of observed $^{134}$Cs (red) and $^{137}$Cs (blue) concentrations from the 2013 CLIVAR P02 transect along 30°N. The sampling longitude is shown on the top axis, and the concentration in Bq/m$^3$ is shown along the bottom axis. The panels are identified with the letters a–m and are shown in west to east order.

their way to producing the spatial homogeneity in $^{134}$Cs concentration in the western North Pacific. Modeling studies support this idea showing that the north-south gradient of tracer across the KE front becomes less pronounced with relatively small range in concentrations after the main plume shifts to the east in winter of 2012 [*Rossi et al.*, 2013, 2014; *Behrens et al.*, 2012; *Garraffo et al.*, 2014].

In 2014, $^{134}$Cs was detected along the MLML transect both in the central Alaskan Gyre and at one of the stations in the vicinity of the California coast (Figure 2C). The MLML transect is situated north of the bifurcation zone of the subtropical gyre in the eastern North Pacific and intersects the Alaska Current, which is a northern branch of the North Pacific Drift. The detection of $^{134}$Cs in the Alaskan gyre was not surprising given observations of the arrival of the Fukushima $^{134}$Cs in 2013 and 2014 in the upper 150 m of the water column along a Canadian repeat sampling Line-P [*Smith et al.*, 2014]. The $^{134}$Cs concentrations of the MLML samples were between 0.6 and 5.4 Bq/m$^3$ and were slightly higher than the 2014 concentration found at westernmost Line-P station P26 at 145°W, 50°N reported as 0.4 to 2.1 Bq/m$^3$ [*Smith et al.*, 2014]. In the eastern North Pacific, numerical models indicate faster currents north of 40°N than to the south of 30°N and therefore predict an earlier arrival of tracer northward along the west coast of Canada and into the Gulf of Alaska than southward along the US coast [*Rossi et al.*, 2013, 2014; *Behrens et al.*, 2012; *Garraffo et al.*, 2014; *Rypina et al.*, 2014]. The fast delivery at higher latitudes explains the detection of $^{134}$Cs at station P26 in 2013 while no evidence of $^{134}$Cs was found east of 160.6°W along 30°N during the same year. One MLML sample, 150 km off the California coast, suggests a surface $^{134}$Cs concentration of 5.4 Bq/m$^3$ (Figure 2C). Unfortunately, the Cs observations are too coarse to resolve the underlying physics explaining this single elevated point. However, likely candidates include processes associated with mesoscale or smaller-scale ocean variability, particularly in the highly eddy-rich California Current region.

## 4. Observed Vertical Cs Distribution

Given that the FNPP $^{134}$Cs/$^{137}$Cs ratio was close to 1 at the time of the accident, and that prior to the FNPP accident $^{134}$Cs levels were below the detection limit, throughout this analysis the difference between the $^{134}$Cs and $^{137}$Cs vertical distributions is attributed to the preexisting background level of $^{137}$Cs due to weapons testing (1.5 to 2 Bq/m$^3$). These background values agree well with the observed near-uniform vertical distribution of $^{137}$Cs concentration east of 160.6°W and are consistent with the nearly constant differences between the observed $^{134}$Cs and $^{137}$Cs profiles (Figure 3). The observation at 30°N suggested that there was no detectable $^{134}$Cs found east of 160.6°W either at the surface or within the observed water column in 2013 (Figures 2B and 3, j–m). West of 175°E (Figure 3, a–e), $^{134}$Cs was observed to penetrate down to 500 m with subsurface $^{134}$Cs maxima at ~300 m for all the profiles. As the plume of contaminated water progresses eastward, near the dateline (Figure 3, f–g), the subsurface maximum is most pronounced at ~150 m depth, but detectable isotope was found to clearly penetrate down to 300 m at all stations west of 177.3°W (Figure 3, a–g). At the eastern edge of the FNPP Cs plume near 160°W, $^{134}$Cs activity was confined to the upper few hundred meters with a weak subsurface maximum at 150 m and no sign of the deeper penetration seen to the west (Figure 3, h–i). Further detail on the $^{134}$Cs vertical structures cannot be captured by the four observed depths available; however, based on these observations it can be concluded that the subsurface maximum in FNPP $^{134}$Cs concentration increases with depth to 300 m and possibly deeper in the western

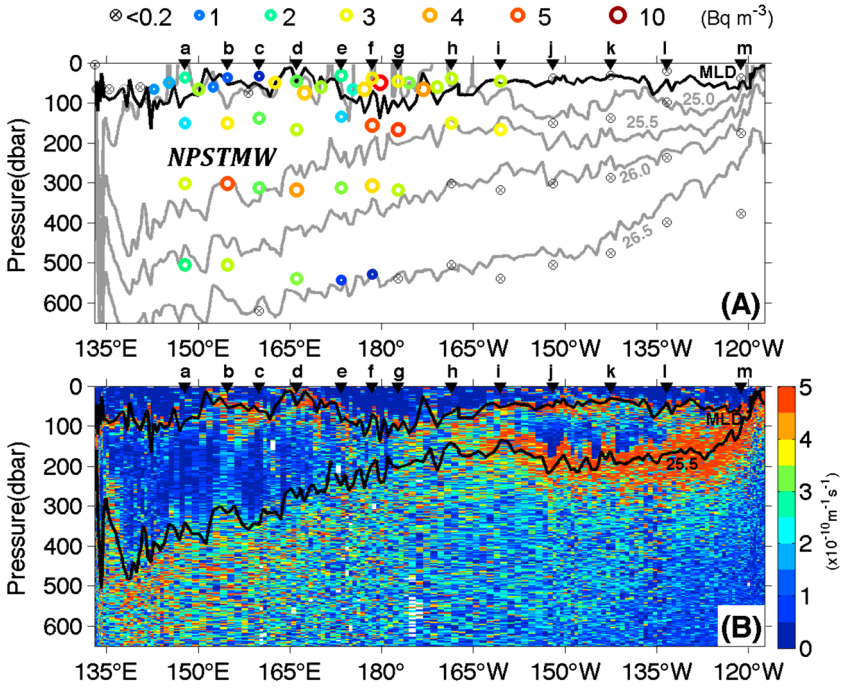


**Figure 4.** (A) Colored circles represent 2013 30°N $^{134}$Cs concentrations in Bq/m$^3$ from the CLIVAR P2 surface and profile samples. Gray contours illustrate the 25.0, 25.5, 26.0, and 26.5$\sigma_\theta$ isopycnal surfaces. Black line denotes MLD. Densities and MLDs are estimated from P02 hydrography (see text). (B) Potential vorticity ($10^{-10}$ m$^{-1}$ s$^{-1}$) along 30°N calculated from the 2013 P02 temperature and salinity fields are shown as colored shading. The two black solid lines denote the MLD (upper curve) and the 25.5$\sigma_\theta$ potential density isopycnal surface (lower curve) both calculated as in Figure 4A. Profile station locations are marked by inverted triangles along the top edge of the figure.

basin and that the depth of penetration shoals toward east. In 2014, the profiles from the northeastern Pacific showed detectable $^{134}$Cs in the upper 250 m (see supporting information Figure S1), with the majority of the $^{134}$Cs confined within the mixed layer, which averages about 150 m in wintertime. With no clear subsurface maxima, this surface intensified $^{134}$Cs structure agrees well with the results of *Smith et al.* [2014].

Taking advantage of the simultaneous temperature and salinity measurements provided by 2013 P02 transect (30°N), density surfaces, and mixed layer depths (MLD) were calculated (Figure 4A) to further elucidate the physical mechanisms responsible for the observed patterns of $^{134}$Cs. Here MLDs (black solid line in Figure 4) are defined as the depths where density has increased by 0.125 kg/m$^3$ over its surface value [*Levitus*, 1982]. At the end of March to May when the P02 expedition was conducted, the zonal mean MLD along the 30°N section was 62 ± 29 m. Consistent with P02 crossing through the center of the North Pacific subtropical gyre at 30°N, the observed density structure is characterized by the shoaling of isopycnal surfaces from west to east. Our first two Cs profiles are located 147.8°E and 154.7°E (Figure 4A, a–b). Here Fukushima $^{134}$Cs penetrates down to at least 500 m, just below 26.0$\sigma_\theta$ (Figure 4A, a–b). With slightly deeper profiles between 165°E and 180°, $^{134}$Cs is found at 600 m slightly above 26.5$\sigma_\theta$ (Figure 4A, d–f). In spite of similarly deep profiles to the east of the dateline, shallower penetration associated with a maximum density of 25.5$\sigma_\theta$ is found between 165°W and 160.6°W (Figure 4A, h–i). No $^{134}$Cs is found east of 160.6°E (Figure 4A, j–m). West of 180°, the only indication of a maximum depth of penetration, available from these observations, is from the deepest sample collected from 160°E (Figure 4A, c) that did not contain detectable levels of $^{134}$Cs. Note also that near the dateline, the depth of $^{134}$Cs penetration depth shoals drastically over a relatively short distance from 26.5$\sigma_\theta$ at 178.4°E (Figure 4A, f) to 26.0$\sigma_\theta$ at 177.3°W (Figure 4A, g) to 25.5$\sigma_\theta$ at 168.6°W (Figure 4A, h).

## 5. Discussion

In the western Pacific, strong wintertime heat loss to the atmosphere results in deep convective mixing south of the KE [*Rainville et al.*, 2014]. This region is the formation site of a distinct water mass known as North Pacific

Subtropical Mode Water (NPSTMW). *Aoyama et al*. [2008] found two cores of the enhanced concentration of the global weapon testing $^{137}$Cs fallout at 20°N along 165°E and showed that these two maxima were colocated in the density space between the NPSTMW and the Lighter Central Mode Water which is formed in the subarctic and transported southward. The subsurface $^{134}$Cs maxima at 500 m south of the KE were reported along meridional transects in the western Pacific from April 2012 to March 2013 [*Kaeriyama et al*., 2014; *Kumamoto et al*., 2014]. *Kaeriyama et al*. [2014] used the apparent oxygen utilization to deduce the timing of this source and suggested that some of the $^{134}$Cs originated from the atmospheric fallout in March 2011. The Fukushima-related $^{134}$Cs was deposited south of the KE or/and transported southward from the FNPP source region and then distributed into the mode water layers via the deep convective mixing that occurred during the winters of 2011 and 2012. In late winter of 2011 to 2014, the deepest MLD was observed to be about 290 to 360 m on average at Kuroshio Extension Observatory (KEO) mooring site at 32.3°N, 144.6°E [e.g., *Tomita et al*., 2010]. In as far as one accepts that the MLDs observed at KEO are representative of western Pacific deep mixing events, the observed deep $^{134}$Cs intrusion to greater than 500 m cannot be fully explained by the wintertime deep convective mixing except perhaps in terms of stronger local storm events. Sporadic local events are, however, unlikely to produce such deep penetration spread along a track 3000 km in length (Figure 4A, a–f).

The distribution of mode waters along the P02 transect is described by the subsurface minima in potential vorticity (PV) associated with strong mixing [*Talley*, 1988] (Figure 4B). The homogeneous low PV waters ($<2.0\times10^{-10}\,\mathrm{m^{-1}\,s^{-1}}$) extend from below the mixed layer down to the 25.5$\sigma_\theta$ isopycnal surface west of the 180°. This isopycnal surface reaches depths of 500 m at 140°E but shoals to 300 m at 180°, which is qualitatively consistent with the behavior of the observed $^{134}$Cs penetration depth (i.e., deepening to the west and shoaling to the east). Note, however, that $^{134}$Cs was observed to have penetrated to a deeper level than the typical NPSTMW layer depth, suggesting that the particular water mass associated with this Cs penetration was denser than the typical NPSTMW.

The deepest $^{134}$Cs penetrations observed between 165°E and 180° were in the density range of the Central Mode Water (CMW), which would imply a connection to the subduction of Cs contaminated waters during CMW formation. The formation region for CMW lies to the north of the Kuroshio Front between 33°N–39°N and ~142°E–160°W [*Oka and Qiu*, 2012], where lighter CMW is subducted into the permanent pycnocline through lateral induction, while denser CMW is entrained into deep mixed layer. However, the time scale for CMW to be transported from the formation region to the western Pacific is estimated to be order of 10 years, even longer for the denser variety CMW [*Suga et al*., 2008], suggesting that the deep $^{134}$Cs observed in 26.5$\sigma_\theta$ barely 3 years after the release is unlikely to be explained by CMW processes.

North Pacific Intermediate Water (NPIW), characterized by salinity minimum water near 26.8$\sigma_\theta$ isopycnal, is another distinct water mass extensively observed in the North Pacific subtropical gyre. Originating in the subarctic, NPIW is formed as a result of fresh surface subarctic water advecting and diffusing along isopycnals into the subtropical circulation at Kuroshio-Oyashio confluence region [*Talley*, 1993; *Qiu*, 1995; *Yasuda et al*., 1996; *Kouketsu et al*., 2007]. Considering the estimated NPIW formation time scale of 1–1.5 years [*Simizu et al*., 2004], the Fukushima Cs discharged near NPIW formation site might have been transported to the middepth subtropical gyre circulation following the NPIW pathways, which may potentially explain the relatively rapid deep penetration of the $^{134}$Cs in our observations.

Another possible mechanism for what appears to be relatively rapid and deep $^{134}$Cs penetration is subduction along the Kuroshio front as suggested by a modeling study of *Garraffo et al*. [2014]. In this numerical experiment, tracers were transported southward across the current front by subduction along the steeply sloping isopycnals, creating a maximum at about 600 m south of the Kuroshio and KE fronts. A more detailed examination on the cause of the rapid and deep penetration of the $^{134}$Cs suggested by the observations between 165°E and the dateline is currently underway and will be reported elsewhere.

## 6. Summary

Here we present analysis of Fukushima-derived cesium observed from water samples collected in the North Pacific from oceanographic transects occupied from 2012 to 2014. The horizontal and vertical distributions of observed Fukushima-derived radionuclides, specifically $^{134}$Cs and $^{137}$Cs, were examined to investigate the

spreading of the radioactive plume and to shed light on the underlying physical processes. The $^{134}$Cs radioisotope, which carries a footprint unique to the FNPP accident, was observed to extend along the 30°N transect to 174.3°W in 2012 and farther east to 160.6°W in 2013, suggesting an eastward propagation speed of ~15° of longitude a year (~5 cm/s). Consistent with the observation location to south of the expected main axis of the plume, the observed eastward spread of $^{134}$Cs along 30°N is slightly slower than the estimates derived based on near-surface drifters [*Rypina et al*., 2014] and the speed predicted by numerical models [*Rossi et al*., 2013, 2014; *Behrens et al*., 2012; *Garraffo et al*., 2014].

Samples collected along the 30°N in 2013 indicated higher surface $^{134}$Cs concentrations in the central Pacific compared to west of 160°E by a few Bq/m$^3$. This pattern suggests that the main body of the $^{134}$Cs plume associated with the major discharge event in early April 2011 was located between 160°E and 160°W in May 2013 with corresponding surface $^{134}$Cs concentrations of 3–5 Bq/m$^3$. No $^{134}$Cs was detected east of 160.6°W as of spring 2013 where the $^{137}$Cs concentrations in the upper 500 m of the water column was a nearly uniform 1–2 Bq/m$^3$, typical of the preexisting weapon testing $^{137}$Cs levels. In 2014, $^{134}$Cs was observed along a transect between Dutch Harbor and Eureka crossing the Alaskan gyre. The appearance of Fukushima Cs at this location agrees well with numerical model and drifter-based predictions [*Rossi et al*., 2013, 2014; *Behrens et al*., 2012; *Garraffo et al*., 2014; *Rypina et al*., 2014] and is consistent with the results reported by *Smith et al*. [2014] along Line-P who observed the arrival of $^{134}$Cs in 2013 in the upper 150 m along the Canadian continental shelf.

Vertical profiles of $^{134}$Cs are few and far between. Our 2013 30°N data set suggests a vertical distribution of $^{134}$Cs characterized by subsurface maxima at all stations west of 160.6°W. The depth of the subsurface maximum and the depth of the deepest $^{134}$Cs penetration were greater in the west and shoaled to the east. As in the surface observations, no $^{134}$Cs was detected east of 160.6°W. West of the dateline, Cs profiles suggest subsurface maxima at 300 m with penetration to 500–550 m (equivalent to 26–26.5$\sigma_\theta$ density surfaces). The penetration depth shoaled rapidly toward the east to 400 m (26.0$\sigma_\theta$) just beyond the dateline, 200 m (25.5$\sigma_\theta$) by 168°W, and completely disappeared by 152°W.

In the west, $^{134}$Cs was observed to reach the NPSTMW layer, implying that the deep $^{134}$Cs penetration could be the result of wintertime convective mixing and the associated mode water formation process. However, some of the observed Cs was located denser and deeper than NPSTMW and thus cannot be explained by the deep convective mixing alone. A number of possible theories were presented, but exactly how Fukushima-derived Cs could be brought down to 600 m within 3 years of the release has yet to be clarified. Numerical model simulations that resolve the frontal-scale dynamics in the KE front will be an important component of future analyses, but to both ground truth these models and to better understand the role of ocean circulation and vertical mixing processes in the spatial distribution and eastward progression of the $^{134}$Cs in the North Pacific, sustained water sampling and hydrographic observations are critical.

**Acknowledgments**

We would like to thank the captains, crews, and science parties of all the cruises in collecting the samples for this research. We would like to thank Steven Pike and Crystaline Breier for their analysis of the cesium isotopes. This work was supported by the grant OCE-1356630 from the National Science Foundation, the Gordon and Betty Moore Foundation (grant GBMF3007), and the Deerbrook Charitable Trust (grant WHOI-DCT#12-12).

The Editor thanks two anonymous reviewers for their assistance in evaluating this paper.

## References

Aoyama, M., and K. Hirose (2004), Artificial radionuclides database in the Pacific Ocean: HAM database, *Sci. World J.*, *4*, 200–215.

Aoyama, M., K. Hirose, K. Nemoto, Y. Takatsuki, and D. Tsumune (2008), Water masses labeled with global fallout $^{137}$Cs formed by subduction in the North Pacific, *Geophys. Res. Lett.*, *35*, L01604, doi:10.1029/2007GL031964.

Aoyama, M., M. Fukasawa, K. Hirose, Y. Hamajima, T. Kawano, P. P. Povinec, and J. A. Sanchez-Cabeza (2011), Cross equator transport of $^{137}$Cs from North Pacific Ocean to South Pacific Ocean (BEAGLE2003 cruises), *Prog. Oceanogr.*, *89*, 7–16.

Aoyama, M., M. Umematsu, D. Tumune, and Y. Hamajima (2013), Surface pathway of radioactive plume of TEPCO Fukushima NPP1 released $^{134}$Cs and $^{137}$Cs, *Biogeosciences*, *10*, 3067–3078, doi:10.5194/bg-10-3067-2013.

Bailly du Bois, P., P. Laguionie, D. Boust, I. Korsakissok, D. Dideir, and B. Fievét (2012), Estimation of marine source-term following Fukushima Dai-ichi accident, *J. Environ. Radioact.*, *114*, 2–9.

Behrens, E., F. U. Schwarzkopf, J. F. Lübbecke, and C. W. Böning (2012), Model simulations on the long-term dispersal of $^{137}$Cs released into the Pacific Ocean off Fukushima, *Environ. Res. Lett.*, *7*, 034004, doi:10.1088/1748-9326/7/3/034004.

Book, J. A., M. Wimbush, S. Imawaki, H. Ichikawa, H. Uchida, and H. Kinoshita (2002), Kuroshio temporal and spatial variations south of Japan determined from inverted echo sounder measurements, *J. Geophys. Res.*, *107*(C9), 3121, doi:10.1029/2001JC000795.

Bowen, V. T., V. E. Noshkin, H. D. Livingston, and H. L. Volchok (1980), Fallout radionuclides in the Pacific Ocean: Vertical and horizontal distributions, largely from GEOSECS stations, *Earth Planet. Sci. Lett.*, *49*, 411–434.

Buesseler, K. O., M. Aoyama, and M. Fukasawa (2011), Impacts of the Fukushima nuclear power plants on marine radioactivity, *Environ. Sci. Technol.*, *45*, 9931–9935.

Buesseler, K. O., et al. (2012), Fukushima-derived radionuclides in the ocean and biota off Japan, *Proc. Natl. Acad. Sci. U.S.A.*, *109*, 5984–5988, doi:10.1073/pnas.1120794109.

Charette, M. A., C. F. Breier, P. B. Henderson, S. M. Pike, I. I. Rypina, S. R. Jayne, and K. O. Buesseler (2013), Radium-based estimates of cesium isotope transport and total direct ocean discharges from the Fukushima Nuclear Power Plant accident, *Biogeosciences*, *10*, 2159–2167, doi:10.5194/bg-10-2159-2013.

Chino, M., H. Nakayama, H. Nagai, H. Terada, G. Katata, and H. Yamazawa (2011), Preliminary estimation of release amounts of $^{131}$I and $^{137}$Cs accidentally discharged from the Fukushima Daiichi Nuclear Power Plant into the atmosphere, *J. Nucl. Sci. Tech.*, *48*, 1129–1134.

Garraffo, Z. D., H.-C. Kim, A. Mehra, T. Spindler, I. Rivin, and H. L. Tolman (2014), Modeling of $^{137}$Cs as a tracer in a regional model for the Western Pacific, after the Fukushima Daiichi Nuclear Power Plant accident of March 2011, *Weather Forecasting*, doi:10.1175/WAF-D-13-00101.1.

Holte, J., and L. Talley (2009), A new algorithm for finding mixed layer depths with applications to argo data and subantarctic mode water formation, *J. Atmos. Oceanic Technol.*, *26*, 1920–1939, doi:10.1175/2009JTECHO543.1.

Imawaki, S., H. Uchida, H. Ichikawa, M. Fukasaw, S. Umatani, and the ASUKA Group (2001), Satellite altimeter monitoring the Kuroshio transport south of Japan, *Geophys. Res. Lett.*, *24*, 17–20, doi:10.1029/2000GL011796.

Inomata, Y., M. Aoyama, and K. Hirose (2009), Analysis of 50-y record of surface $^{137}$Cs concentrations in the global ocean using the HAM-global database, *J. Environ. Monit.*, *11*(1), 116–125.

Kaeriyama, H., et al. (2014), Southwest intrusion of $^{134}$Cs and $^{137}$Cs derived from the Fukushima Dai-ichi nuclear power plant accident in the Western North Pacific, *Environ. Sci. Technol.*, *48*, 3120–3127.

Kamenik, J., H. Dulaiova, F. Sebesta, and K. Stastna (2013), Fast concentration of dissolved forms of cesium radioisotopes from large seawater samples, *J. Radioanal. Nucl. Chem.*, *296*, 841–846.

Kanda, J. (2013), Continuing $^{137}$Cs release to the sea from the Fukushima Dai-ichi Nuclear Power Plant through 2012, *Biogeosciences*, *10*, 6107–6113, doi:10.5194/bg-10-6107-2013.

Kouketsu, S., I. Yasuda, and Y. Hiroe (2007), Three-dimensional structure of frontal waves and associated salinity minimum formation along the Kuroshio Extension, *J. Phys. Oceanogr.*, *37*, 644–656.

Kumamoto, Y., M. Aoyama, Y. Hamajima, T. Aono, S. Kouketsu, A. Murata, and T. Kawano (2014), Southward spreading of the Fukushima-derived radiocesium across the Kuroshio Extension in the North Pacific, *Sci. Rep.*, *4*, 4276, doi:10.1038/srep04276.

Levitus, S. (1982), *Climatological Atlas of the World Ocean*, *NOAA Prof. Pap.*, vol. 13, 173 pp., U.S. Gov. Print. Off., Washington, D. C.

Macdonald, A. M., S. Mecking, J. M. Toole, P. E. Robbins, G. C. Johnson, S. E. Wiffels, L. D. Talley, and M. Cook (2009), The WOCE-era 3-D Pacific Ocean circulation and heat budget, *Prog. Oceanogr.*, *82*, 281–325.

Masumoto, Y., Y. Miyazawa, D. Tsumune, T. Kobayashi, C. Estournel, P. Marsaleix, L. Lanerolle, A. Mehra, and Z. D. Garraffo (2012), Oceanic dispersion simulation of Cesium 137 from Fukushima Daiichi Nuclear Power Plant, *Elements*, *8*, 207–212.

Miyazawa, Y., Y. Masumoto, S. M. Varlamov, T. Miyama, M. Takigawa, M. Honda, and T. Saino (2013), Inverse estimation of source parameters of oceanic radioactivity dispersion models associated with the Fukushima accident, *Biogeosciences*, *10*, 2349–2363.

Nagao, S., M. Kanamori, S. Ochiai, S. Tomihara, K. Fukushi, and M. Yamamoto (2013), Export of $^{134}$Cs and $^{137}$Cs in the Fukushima river systems at heavy rains by Typhoon Roke in September 2011, *Biogeosciences*, *10*, 6215–6223.

Oka, E., and B. Qiu (2012), Progress of North Pacific mode water research in the past decade, *J. Oceanogr.*, *68*, 5–20, doi:10.1007/s10872-011-0032-5.

Pike, S. M., K. O. Buesseler, C. F. Breier, H. Dulaiova, K. Stastna, and F. Sebesta (2013), Extraction of cesium in seawater off Japan using AMP-PAN resin and quantification via gamma spectroscopy and inductively coupled mass spectrometry, *J. Radioanal. Nucl. Chem.*, *296*, 369–374, doi:10.1007/s10967-012-2014-5.

Qiu, B. (1995), Why is the North Pacific Intermediate Water confined on density surfaces around $\sigma_\theta = 26.8$?, *J. Phys. Oceanogr.*, *25*, 168–180.

Rainville, L., S. R. Jayne, and M. F. Cronin (2014), Variations of the North Pacific subtropical mode water from direct observations, *J. Clim.*, *27*, 2842–2860, doi:10.1175/JCLI-D-13-00227.1.

Rossi, V., E. V. Sebille, A. S. Gupta, V. Garçon, and M. H. England (2013), Multi-decadal projections of surface and interior pathways of the Fukushima cesium-137 radioactive plume, *Deep Sea Res., Part I*, *80*, 37–46.

Rossi, V., E. V. Sebille, A. S. Gupta, V. Garçon, and M. H. England (2014), Corrigendum to "Multi-decadal projections of surface and interior pathways of the Fukushima Cesium-137 radioactive plume" [Deep-Sea Res. I 80 (2013) 37–46], *Deep Sea Res., Part I*, *93*, 162–164.

Rypina, I. I., S. R. Jayne, S. Yoshida, A. M. Macdonald, E. Douglass, and K. O. Buesseler (2013), Short-term dispersal of Fukushima-derived radionuclides off Japan: Modeling efforts and model-data intercomparison, *Biogeosciences*, *10*, 1517–1550, doi:10.5194/bgd-10-1517-2013.

Rypina, I. I., S. R. Jayne, S. Yoshida, A. M. Macdonald, and K. O. Buesseler (2014), Drifter-based estimate of the 5-year dispersal of Fukushima-derived radionuclides, *J. Geophys. Res. Oceans*, *119*, 8177–8193, doi:10.1002/2014JC010306.

Šebasta, F., and V. Štefula (1990), Composite ion exchanger with ammonium molybdophosphate and its properties, *J. Radioanal. Nucl. Chem.*, *140*, 14–21.

Simizu, Y., T. Iwao, I. Yasuda, S. Ito, T. Watanabe, K. Uehara, N. Shikama, and T. Nakano (2004), Formation process of North Pacific Intermediate Water revealed by profiling floats set to drift on 26.7$\sigma_\theta$ isopycnal surface, *J. Oceanogr.*, *60*, 453–462.

Smith, J. N., R. M. Brown, W. J. Williams, M. Robert, R. Nelson, and S. B. Moran (2014), Arrival of the Fukushima radioactivity plume in North American continental waters, *Proc. Natl. Acad. Sci. U.S.A.*, doi:10.1073/pnas.1412814112.

Stohl, A., P. Seibert, G. Wotawa, D. Arnold, J. F. Burkhart, S. Eckhardt, C. Tapia, A. Vargas, and T. J. Yasunari (2012), Xenon-133 and caesium-137 releases into the atmosphere from the Fukushima Dai-ichi Nuclear Power Plant: Determination of the source term, atmospheric dispersion, and deposition, *Atmos. Chem. Phys.*, *12*, 2313–2343.

Suga, T., Y. Aoki, H. Saito, and K. Hanawa (2008), Ventilation of the North Pacific subtropical pycnocline and mode water formation, *Prog. Oceanogr.*, *77*, 285–297.

Talley, L. D. (1988), Potential vorticity distribution in the North Pacific, *J. Phys. Oceanogr.*, *27*, 89–106.

Talley, L. D. (1993), Distribution and formation of North Pacific Intermediate Water, *J. Phys. Oceanogr.*, *23*, 517–537.

Tomita, H., S. Kako, M. F. Cronin, and M. Kubota (2010), Preconditioning of the wintertime mixed layer at the Kuroshio Extension Observatory, *J. Geophys. Res.*, *115*, C12053, doi:10.1029/2010JC006373.

Tsumune, D., T. Tsubone, M. Aoyama, and K. Hirose (2012), Distribution of oceanic $^{137}$Cs from the Fukushima Daiichi Nuclear Power Plant simulated numerically by a regional ocean model, *J. Environ. Radioact.*, *111*, 100–108, doi:10.1016/j.jenvrad.2011.10.007.

United Nations (2000), Exposures to the public form man-made sources of radiation, in *Sources and Effects of Ionizing Radiation. United Nations Scientific Committee on the Effects of Atomic Radiation*, *UNSCEAR 2000 Rep. Gen. Assem., Sci. Annexes*, vol. 1, pp. 158–291, United Nations, New York.

Worthington, L. V., and H. Kawai (1972), Comparison between deep sections across the Kuroshio and the Florida Current and Gulf Stream, in *Kuroshio—Its Physical Aspects*, edited by H. Stommel and K. Yoshida, pp. 371–385, Univ. Tokyo Press, Tokyo.

Yasuda, I., K. Okuda, and Y. Shimizu (1996), Distribution and modification of North Pacific Intermediate Water in the Kuroshio-Oyashio interfrontal zone, *J. Phys. Oceanogr.*, *26*, 448–465.

Yoshida, N., and J. Kanda (2012), Tracking the Fukushima radionuclides, *Science*, *336*, 1115–1116, doi:10.1126/science.1219493.